EUROPEAN ORGANIZATION FOR NUCLEAR RESEARCH

L3 Note 2589
July 7, 2000.

Inclusive K^0_S Meson Production in Two-Photon Collisions

The L3 Collaboration

Abstract

The inclusive production of K^0_S mesons in the reaction $e^+e^- \to e^+e^- hadrons$ is studied with the L3 detector at LEP. Data were collected at centre-of-mass energies from 189 GeV to 202 GeV for a total integrated luminosity of 410 pb^{-1}. The differential cross sections as a function of the transverse momentum and of the pseudorapidity of the K^0_S are measured. The results are compared to the predictions of PHOJET and PYTHIA Monte Carlo models and to perturbative next-to-leading order QCD calculations.

Submitted to the
XXXth International Conference on High Energy Physics
Osaka, Japan, July 27 - August 2, 2000.

1 Introduction

Electron-positron storage rings are a good laboratory to investigate the production of hadrons in two-photon interactions via the process $e^+e^- \to e^+e^- hadrons$. The outgoing electron and positron carry nearly the full beam energy and their transverse momenta are usually so small that they are not detected. The four momentum squared of the two photons is therefore very small ($Q^2 \simeq 0$) and they can be considered to be quasi real.

Photons can interact as pointlike particles (Fig. 1(a)). As shown in Fig. 1(b), a photon can also fluctuate into a vector meson (ρ, Φ, ω, ...) and the two-photon interaction can be modeled by assuming the interaction between two vector mesons (VDM model). This process dominates soft interactions. In leading order Quantum Chromodynamics (QCD), three different processes contribute to the hard interaction of two photons: the direct (Fig. 1(a)), the double-resolved (Fig. 1(c)) and the single-resolved (Fig. 1(d)). In the single and double-resolved processes, the structure of the photon is resolved into partons (quarks and gluons) that take part in the interaction. The probability of finding a parton in the photon carrying a certain fraction of its momentum is parametrized by parton density functions.

The study of single particle production in two-photon hadronic collisions allows to test leading-order and next-to-leading order (NLO) QCD predictions [1], complementing similar studies such as jet production [2].

The production of K^0_S in untagged two-photon collisions has previously been studied by TOPAZ [3] and OPAL [4].

In this paper a study of the inclusive production of K^0_S mesons in untagged two-photon collisions is presented. Data have been collected by the L3 detector at LEP during the years 1998 and 1999 at e^+e^- center-of-mass energies from 189 to 202 GeV corresponding to a total integrated luminosity of 410 pb^{-1}.

The analysis described in this paper is mainly based on the central tracking system. The L3 detector is described in detail elsewhere [5]. The events used in this analysis are collected predominantly by the charged particle track triggers [6].

The $\gamma\gamma \to hadrons$ processes are simulated with the PHOJET [1)] [7] and PYTHIA [2)] [8] event generators. Only the events with $W_{\gamma\gamma} > 10$ GeV and $Q^2 < 8$ GeV^2 are considered, where $W_{\gamma\gamma}$ is the effective mass and Q^2 is the maximum four-vector squared of the two photons.

For the annihilation processes $e^+e^- \to hadrons(\gamma)$, ZZ($\gamma$), Zee($\gamma$), We$\nu$($\gamma$) events are simulated using PYTHIA [8]; KORALZ [9] is used for $e^+e^- \to \tau^+\tau^-(\gamma)$ and KORALW [10] for $e^+e^- \to W^+W^-$. For the $e^+e^- \to e^+e^-\tau^+\tau^-$ channel the generator DIAG36 [11] is used. The events are simulated in the L3 detector using GEANT [12] and GEISHA [13] programs and passed through the same reconstruction program as the data.

2 Event Selection

Hadronic two-photon events are selected by the following criteria :

- At least six particles must be detected. A particle can be a track, a photon or a pion cluster in the hadron calorimeter or in the luminosity monitor. A track must have a transverse momentum $p_t > 100$ MeV, at least 12 wire hits and a distance of closest approach to the nominal vertex less than 10 mm in the transverse plane. A photon

[1)]PHOJET version1.05c

[2)]PYTHIA version 5.718 and JETSET version 7.408

candidate is a cluster in the electromagnetic calorimeter, with no nearby track in a 200 mrad cone, the associated energy in the hadron calorimeter must be smaller than 20% of the electromagnetic energy. Clusters in the hadron calorimeter, without any track within a 300 mrad cone and with an energy greater than 20% of the electromagnetic energy are considered as pions, since they are mainly outside the track chamber detection region. Clusters in the luminosity monitor with energy less than 30 GeV are considered as pions if their energy is below 5 GeV and as photons above 5 GeV.

- The total energy in the electromagnetic calorimeter is required to be greater than 500 MeV in order to suppress beam-gas and beam-wall backgrounds and smaller than 50 GeV, to exclude events from the process $e^+e^- \to \gamma Z$. The total energy deposited in the calorimeters must be less than 40 % of the centre of mass energy, to exclude annihilation events.

- An anti-tag condition is imposed which excludes events with clusters having energy greater than 70 GeV in the luminosity monitor, in a fiducial region of 33–64 mrad. The Q^2 value of the selected events is thus less than 8 GeV^2, its average value being $< Q^2 > \sim 1.5$ 10^{-2}GeV^2.

The visible effective mass of the event is calculated from the four-momentum vectors of the measured particles:

$$W_{\text{vis}}^2 = (\sum_i E_i)^2 - (\sum_i \vec{p}_i)^2 \qquad i = \text{pions, photons}$$

This analysis is limited to events with $W_{\text{vis}} \geq 10$ GeV (Fig. 2).

Once hadronic two-photon events are selected, K^0_S candidates are searched for by reconstructing the secondary vertex produced by the decay $K^0_S \to \pi^+\pi^-$. The following selection criteria are applied to the reconstructed secondary vertices:

- The distance between the secondary vertex and the e^+e^- interaction point must be greater than 3 mm in the transverse plane.

- The angle between the flight direction of the K^0_S candidate (taken as the line between the interaction point and the secondary vertex in the transverse plane) and the total transverse momentum vector of the two outgoing tracks must be less than 0.075 rad.

After all these selection criteria 516540 are selected.

The background from beam-gas and beam-wall interactions is found to be negligible. The background to the process $\gamma\gamma \to hadrons$ is below 1% at low masses, dominated by two-photon τ production. It increases at high masses, due mainly to annihilation processes and reaches a maximum of $\simeq$ 15% at 130 GeV. Considering the K^0_S signal, the background due to non two-photon fusion processes is estimated to be negligible.

In Fig. 3 the $\pi^+\pi^-$ mass spectrum is shown for different intervals of the transverse momentum of the K^0_S candidate. A clear K^0_S signal is present over a smooth background. The width of the signal is found to be $\sigma = 8$ MeV for p_t below 1 GeV. It increases up to $\sigma = 13$ MeV for p_t around 4 GeV, consistent with the Monte Carlo. In Fig. 4 and in Fig. 5 the distributions are shown for the transverse momentum p_t and the pseudorapidity $\eta = -\log(\tan\theta/2)$ of the K^0_S candidates selected in a mass window of $\pm$ 30 MeV around the K^0_S mass.

3 Data Analysis

The differential cross section as a function of p_t is measured in the range $|\eta| < 1.5$ and the differential cross section as a function of $|\eta|$ is measured for $p_t > 1.5$ GeV.

The K^0_S candidates with $|\eta| < 1.5$ are subdivided in 9 bins of p_t with sufficient statistics in each bin. The differential cross section $(d\sigma/dp_t)_i$ is measured for every bin according to the formula:

$$\left(\frac{d\sigma}{dp_t}\right)_i = \frac{(N_{obs} - N_{bkg})_i}{\varepsilon_i \cdot \mathcal{L} \cdot \Delta p_t^i} \tag{1}$$

where i indicates the bin, $(N_{obs} - N_{bkg})_i$ is the number of K^0_S in the bin, ε_i the total detection efficiency, $\mathcal{L}$ the integrated luminosity and Δp_t^i the width of the bin. $(N_{obs} - N_{bkg})_i$ is evaluated by fitting the mass spectrum with a gaussian and a third order Chebyshev polynomial for the background. The total detection efficiency ε_i includes the effects of the acceptance, selection cuts, trigger and corrects for the branching fraction of the K^0_S into $\pi^+\pi^-$. The effects of the detector acceptance and the selection cuts are evaluated by Monte Carlo. The trigger efficiency is evaluated directly from the data; a value of 85% is obtained. In Fig. 6 the total detection efficiency is shown as a function of p_t for the PHOJET and the PYTHIA Monte Carlos. The values obtained with the PHOJET Monte Carlo are used for the measurement of the differential cross section. The difference between the two Monte Carlos is taken as a systematic error (from 2% up to 7%). Other sources of systematic errors are the trigger efficiency (3%) and the selection criteria (6%). In all the figures the statistical and the systematic errors are added in quadrature.

The differential cross section is first measured for the two data samples collected in 1998 and in 1999 separately. The 1998 data sample corresponds to 177 pb^{-1}collected at $\sqrt{s} = 189$ GeV and the 1999 one to 233 pb^{-1}collected at $\sqrt{s} = 191.6 - 202$ GeV. Fig. 7 shows very good agreement between the two measurements. The two data samples will therefore be considered as a single data sample for the rest of this paper.

In Fig. 8 the cross section as a function of the transverse momentum is shown for the whole data sample and is compared to the results published by OPAL [4]. Good agreement is found between the two measurements. L3 data cover also the p_t region below 1 GeV. The cross section shows an exponential behavior at low p_t, typical of the soft interactions [14]. From the exponential fit in the range $0.4 < p_t < 2$ GeV (Fig. 8) the value $< p_t >= 357 \pm 8$ MeV is obtained. The χ^2 is found to be 3.1 for 3 degrees of freedom. At high p_t data are higher than the exponential due to the hard interactions of the two photons.

In order to measure the differential cross section as a function of the pseudorapidity, the same procedure (Eq. 1)is adopted. The K^0_S candidates with $p_t > 1.5$ GeV are subdivided in four bins of $|\eta|$. Fig. 9 shows the total detection efficiency ε_j as a function of $|\eta|$. Also in this case the PHOJET Monte Carlo is used for correcting the data and the difference between the two Monte Carlos is taken as a systematic error.

4 Results

In Fig. 10 and Fig. 11 the differential cross sections are compared to the leading order (LO) predictions of the PHOJET and PYTHIA Monte Carlos. The shape of the $|\eta|$ distribution is well in agreement with PHOJET. PYTHIA is $\sim 20\%$ too low. The p_t distribution is not well reproduced by both the Monte Carlo models.

In Fig. 12 and in Fig. 13 the measured cross sections are compared to the next-to-leading order (NLO) QCD predictions by B.A. Kniehl [1]. The parton density functions of L.E. Gordon and J.K. Storrow [15] are used in the calculation. The factorization and the renormalization scales are set equal to xp_t with $x = 0.5$, 1 and 2. Data at $p_t > 2$ GeV are higher than the theoretical NLO QCD predictions. The direct process (Fig. 1(a)) is insufficient to describe the data.

In order to take the VDM contribution (Fig. 1(b)) into account, the exponential obtained from the fit shown in Fig. 8 can be added to the NLO QCD predictions. The results are shown in Fig. 14. A better agreement is found at high p_t.

5 Conclusions

The inclusive production of K^0_S mesons in the reaction $\mathrm{e^+e^-} \rightarrow \mathrm{e^+e^-}\,hadrons$ is studied with the L3 detector at LEP. Data were collected at centre-of-mass energies from 189 GeV to 202 GeV for a total integrated luminosity of 410 pb^{-1}. The measured differential cross sections as a function of the transverse momentum and of the pseudorapidity of the K^0_S are compared to PHOJET and PYTHIA Monte Carlos and to NLO QCD calculations.

Acknowledgements

We would like to acknowledge B. A. Kniehl for providing the NLO QCD calculations and for the useful discussions.

References

[1] J. Binnewies, B. A. Kniehl and G. Kramer, *Phys. Rev.* **D 53** (1996) 3573;
B. A. Kniehl private communication.

[2] OPAL Collab., G. Abbiendi et al., *Eur. Phys. J.* **C 10** (1999) 547 and references therein.

[3] TOPAZ Collab., R. Enomoto, *Phys. Lett.* **341 B** (1994) 238.

[4] OPAL Collab., K. Ackerstaff et al., *Eur. Phys. J.* **6 C** (1999) 253.

[5] L3 Collab., B. Adeva et al., *Nucl. Inst. Meth.* **A 289** (1990) 35;
L3 Collab., O. Adriani et al., *Phys. Rep.* **236** (1993) 1.

[6] P. Béné et al., *Nucl. Inst. Meth.* **A 306** (1991) 150;
D. Haas et al.,*Nucl. Inst. Meth.* **A 420** (1999)101.

[7] R. Engel, Z. Phys. **C 66** (1995) 203 ;
R. Engel and J. Ranft, *Phys. Rev.* **D 54** (1996) 4246;
R. Engel private communication.

[8] T. Sjöstrand, Comput. Phys. Commun. **82** (1994) 74.

[9] S. Jadach,B. F. L. Ward and Z. Was, Comput. Phys. Commun. **79** (1994) 503.

[10] M. Skrzypek, S. Jadach,W. Placzek, and Z. Was, Comput. Phys. Commun. **94** (1996) 216.

[11] F. A. Berends,P. H. Daverfeldt and R. Kleiss, *Nucl. Phys.* **B 253** (1985) 441.

[12] R. Brun et al., GEANT 3.15 preprint CERN DD/EE/84-1 (Revised 1987).

[13] H. Fesefeldt, RWTH Aachen report PITHA 85/2 (1985). Comput. Phys. Commun. **79** (1994) 503.

[14] A. Zieminski, *"Multiparticle production"*, proceedings of the 1977 European Conference on Particle Physics.

[15] L. E. Gordon and J. K. Storrow, *Nucl. Phys.* bf B 489 (1997) 405.

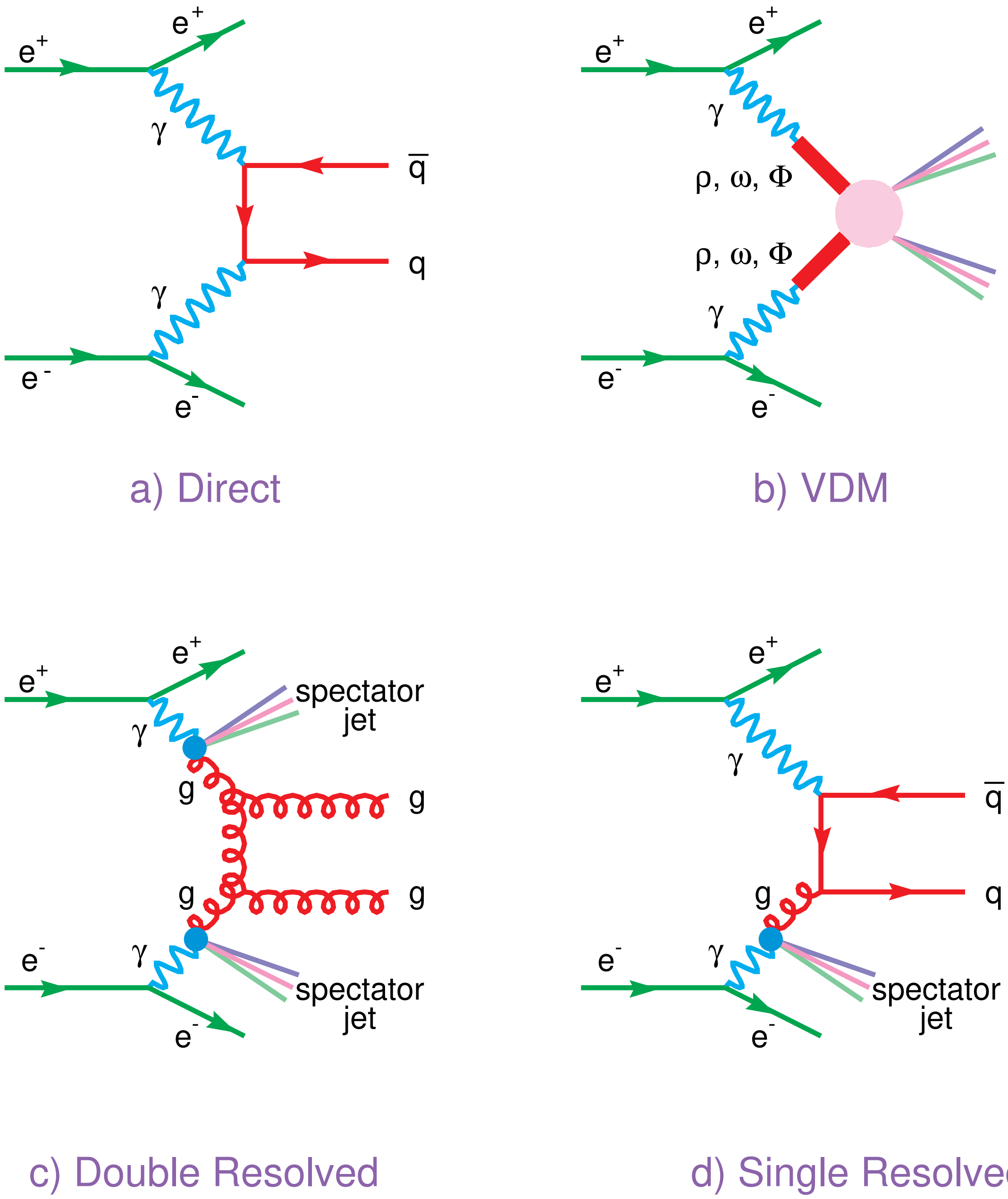

Figure 1: Four different contributions to the process $e^+e^- \to e^+e^- hadrons$.

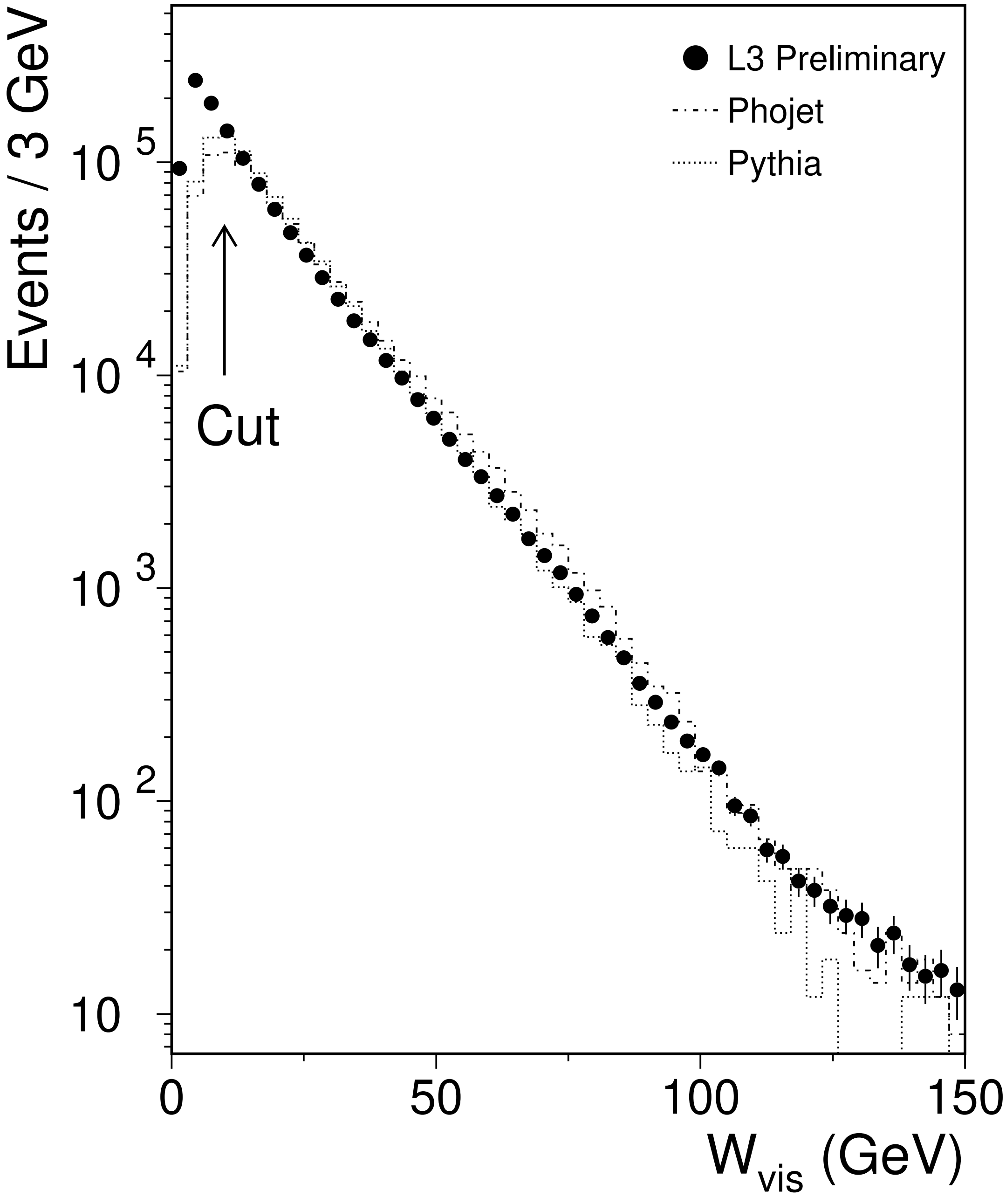

Figure 2: The distribution of the visible effective mass W_{vis}. Only the events with $W_{vis} > 10$ GeV are considered. For the Monte Carlo only the events with $W_{\gamma\gamma} > 10$ GeV are considered.

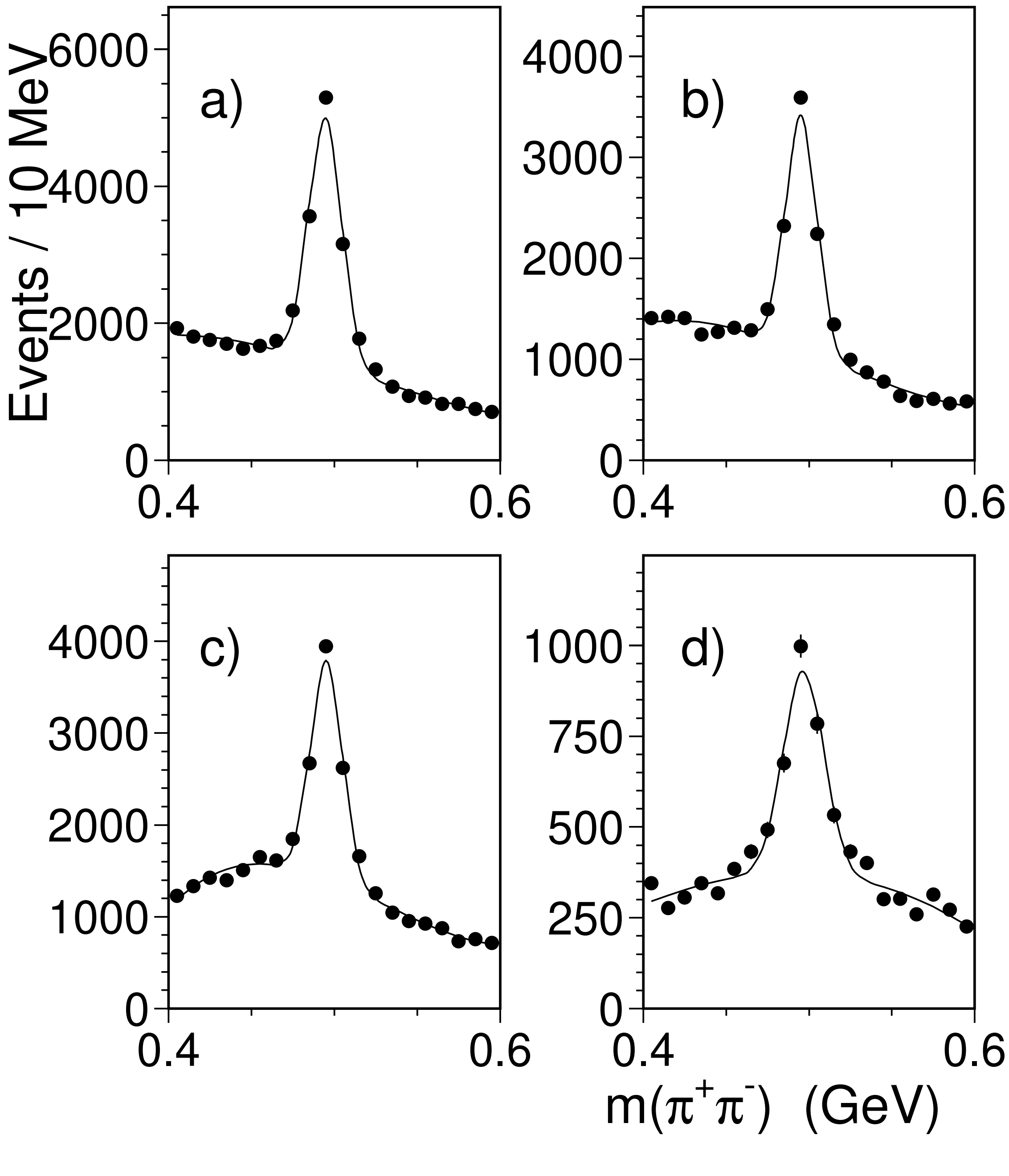

Figure 3: The $\pi^+\pi^-$ mass distribution for different values of the transverse momentum p_t of the K_S^0 candidates: $0.6 < p_t < 0.8$ GeV (a), $0.8 < p_t < 1.0$ GeV (b), $1.0 < p_t < 1.5$ GeV (b) and $1.5 < p_t < 2.0$ GeV (d). The K_S^0 signal is very prominent over a smooth background. The line corresponds to the fit of a gaussian plus a third order Chebyshev polynomial for the background.

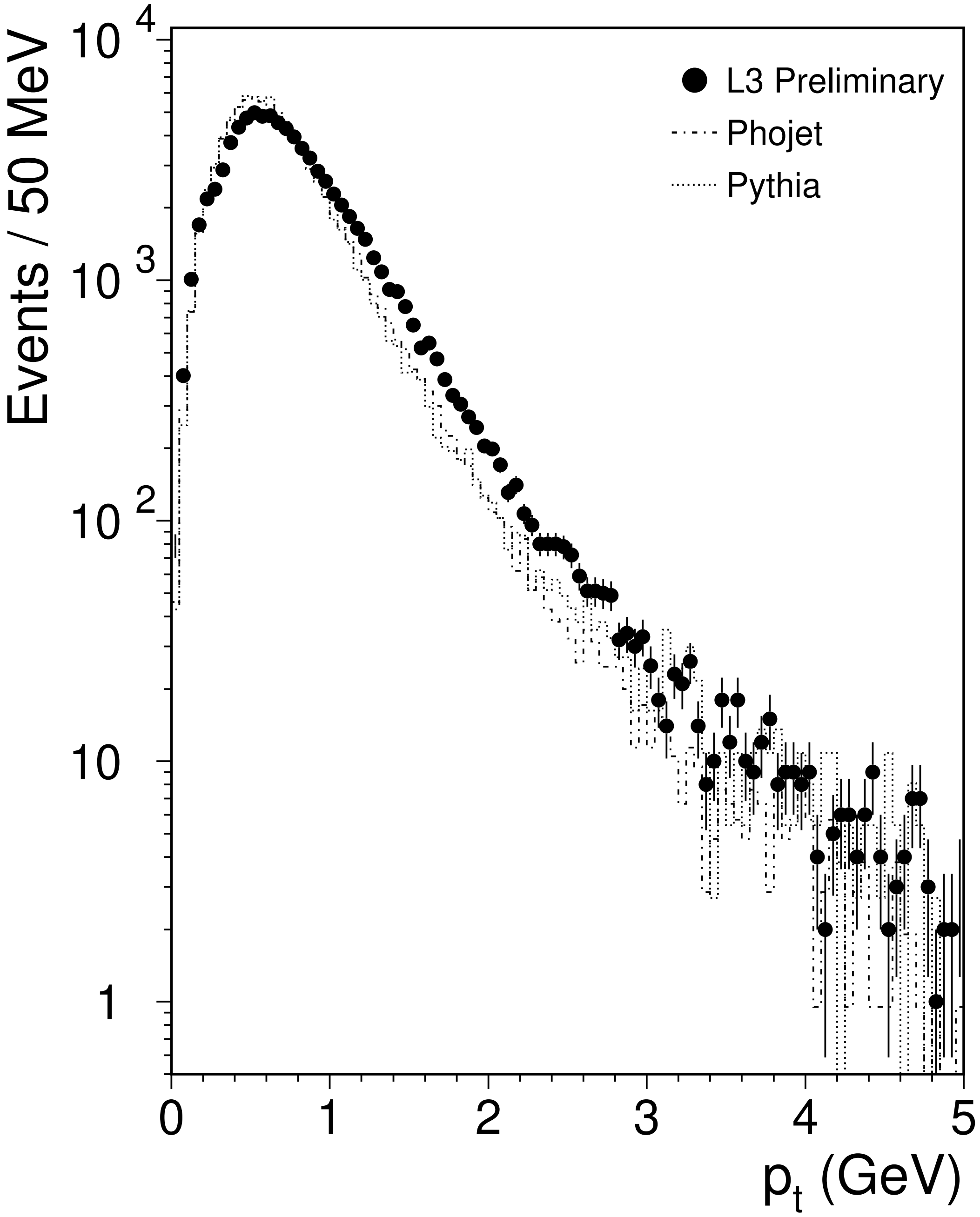

Figure 4: The transverse momentum distribution of the K_S^0 candidates in a mass window of ± 30 MeV around the K_S^0 mass.

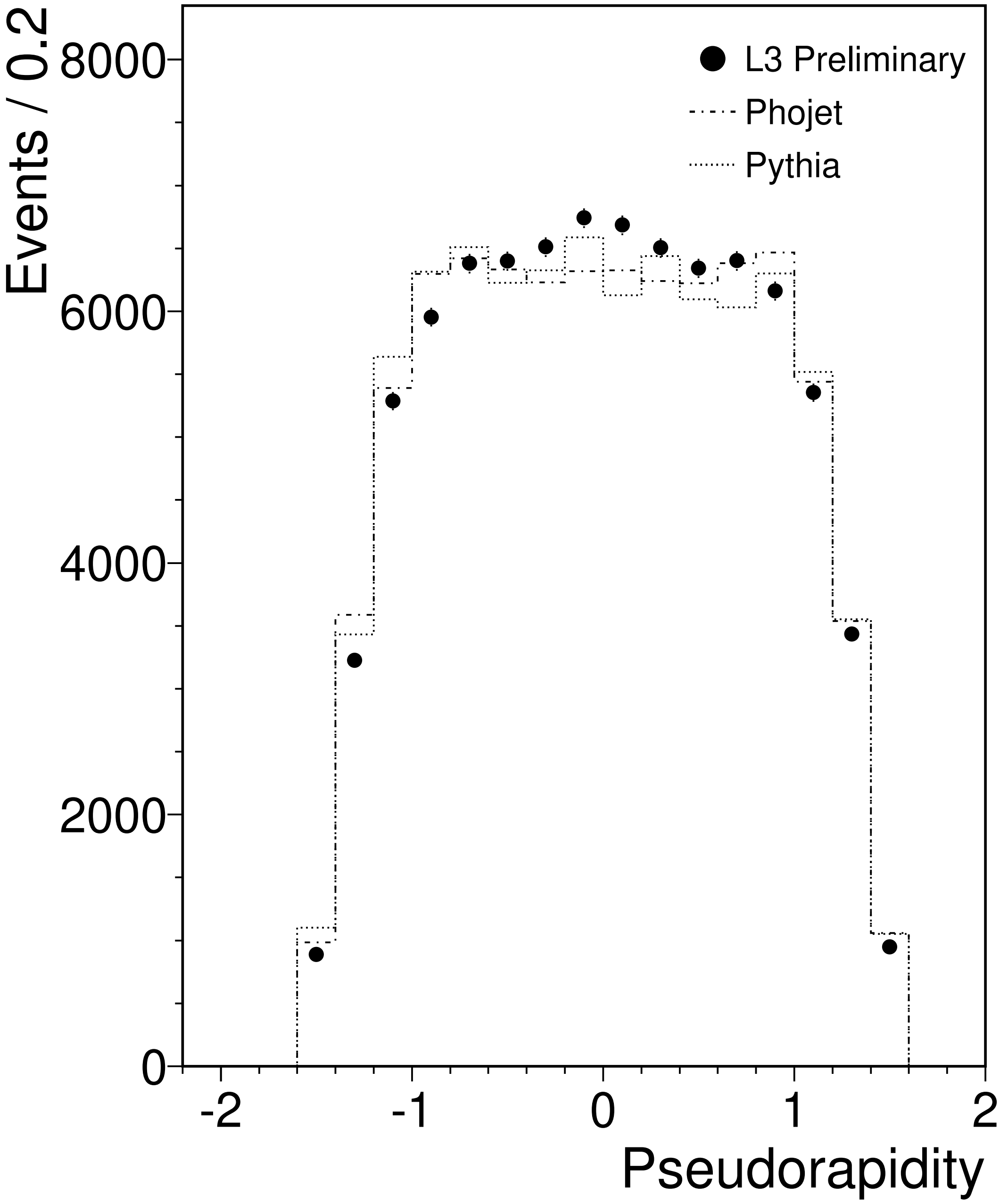

Figure 5: The pseudorapidity distribution of the K^0_S candidates in a mass window of ± 30 MeV around the K^0_S mass.

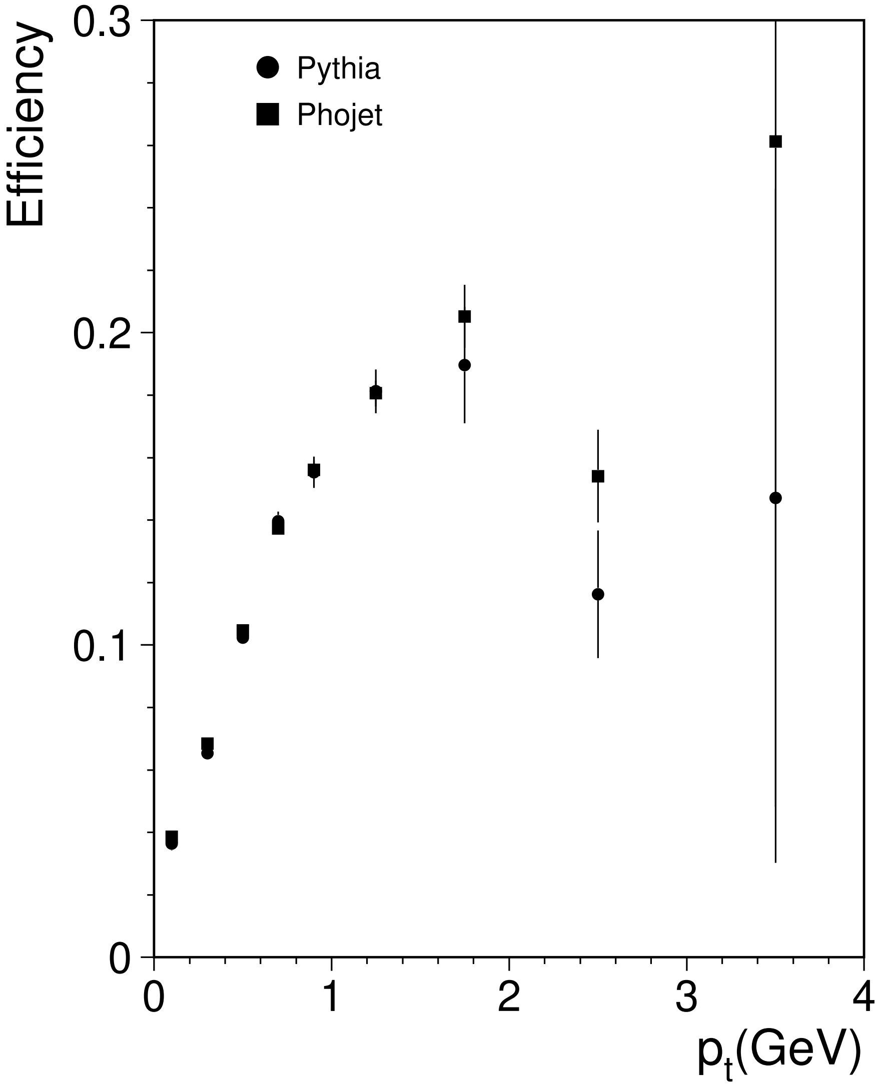

Figure 6: The total detection efficiency as a function of p_t for events with $|\eta| < 1.5$.

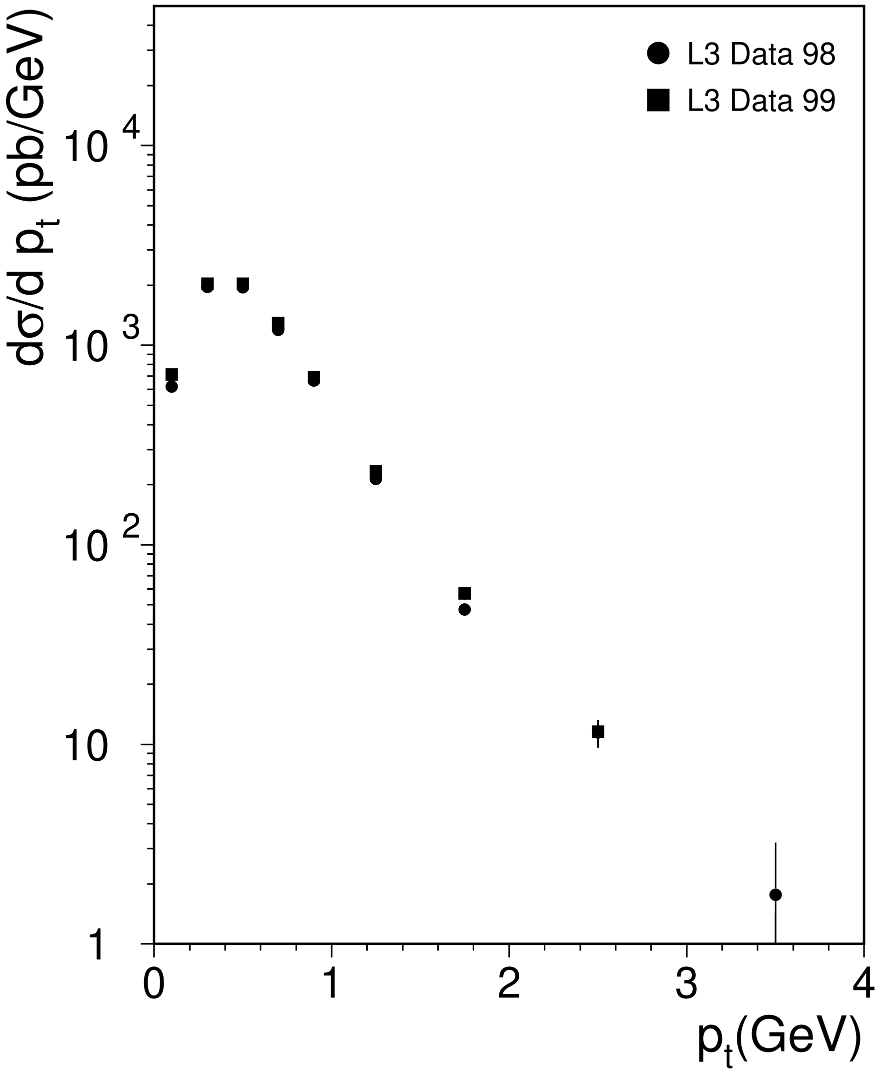

Figure 7: The differential cross section as a function of p_t for $|\eta| < 1.5$ for the 1998 and the 1999 data samples separately.

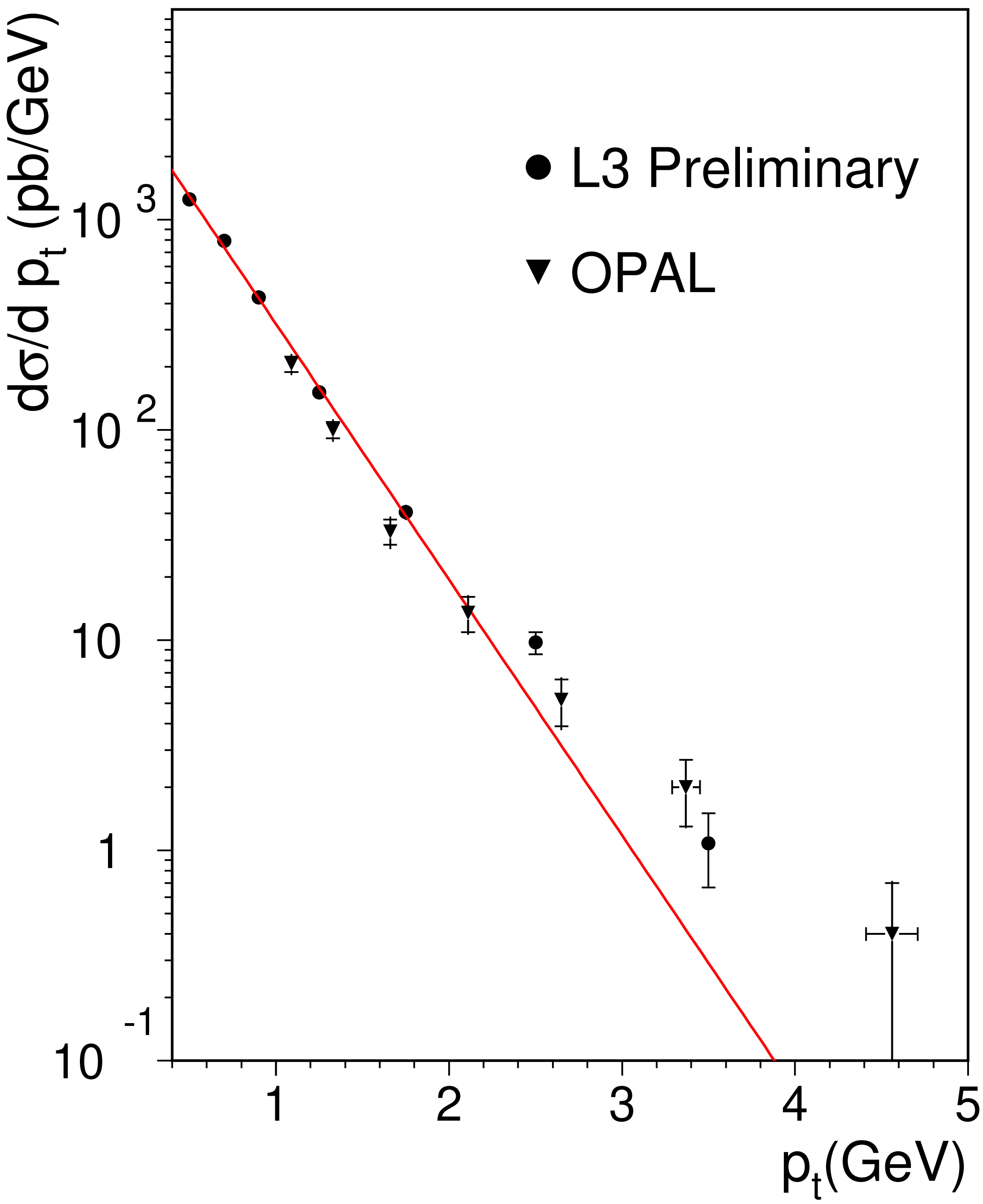

Figure 8: The measured differential cross section as a function of p_t for $|\eta| < 1.5$ is compared to OPAL data. The line corresponds to the exponential fit performed in the interval $0.4 < p_t < 2$ GeV.

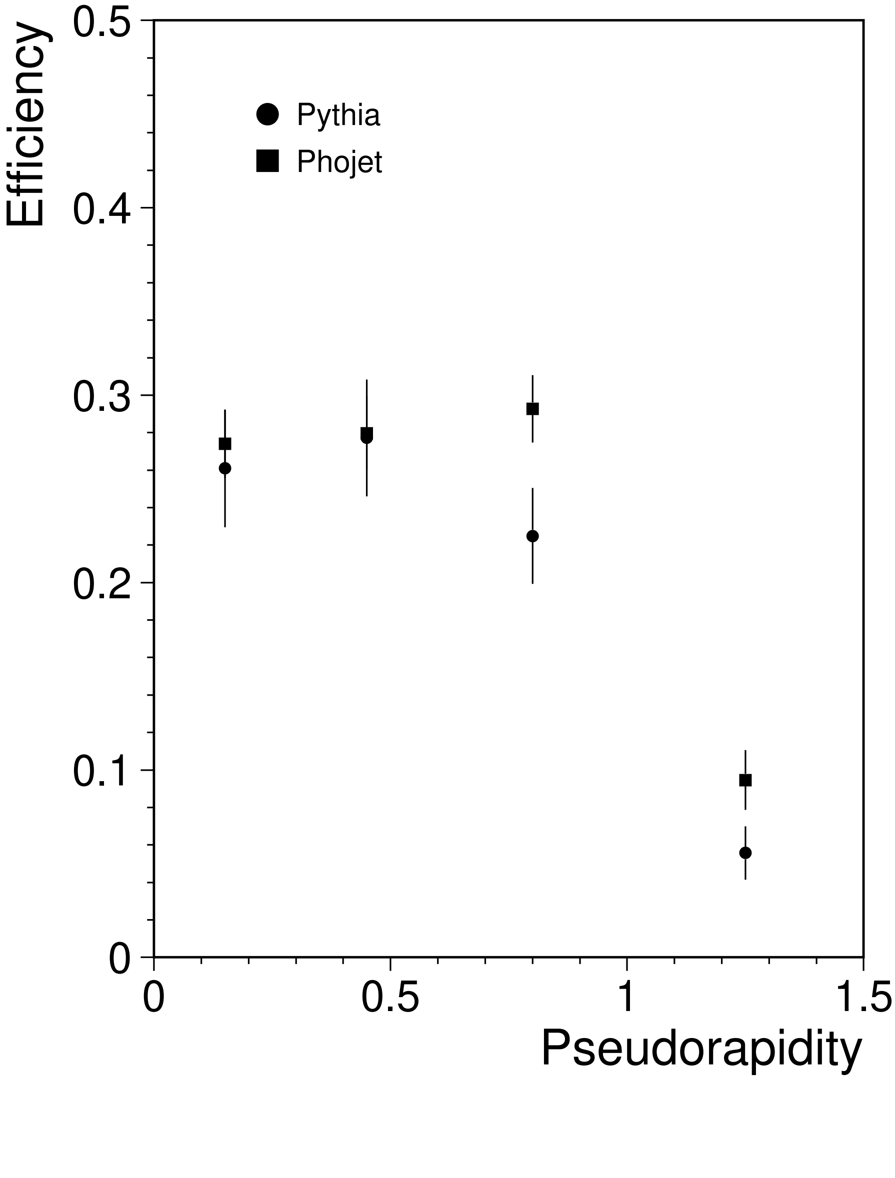

Figure 9: The total detection efficiency as a function of $|\eta|$ for events with $p_t > 1.5$ GeV.

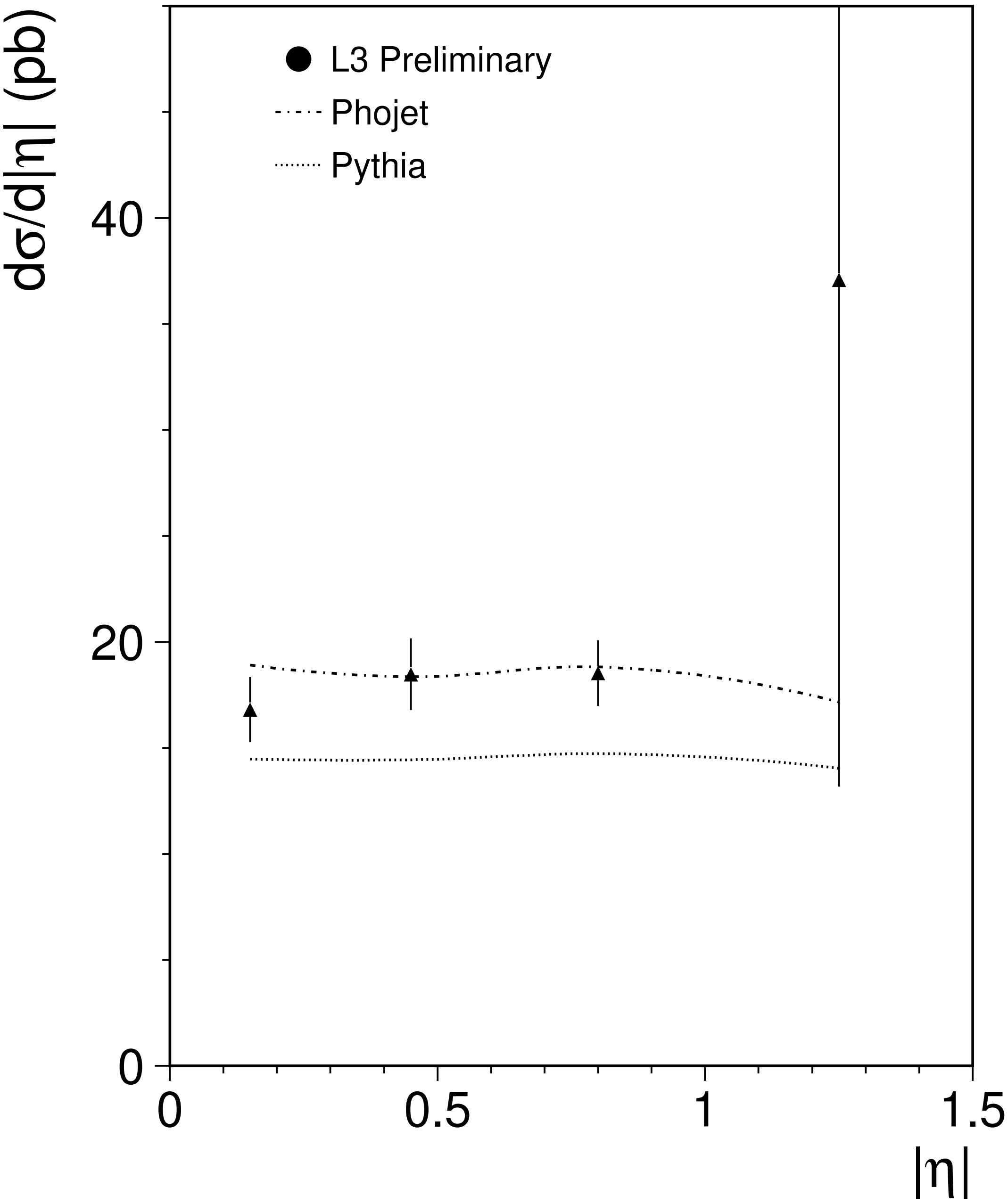

Figure 10: The measured differential cross section as a function of $|\eta|$ for $p_t > 1.5$ GeV is compared to the predictions of the PHOJET and PYTHIA Monte Carlos.

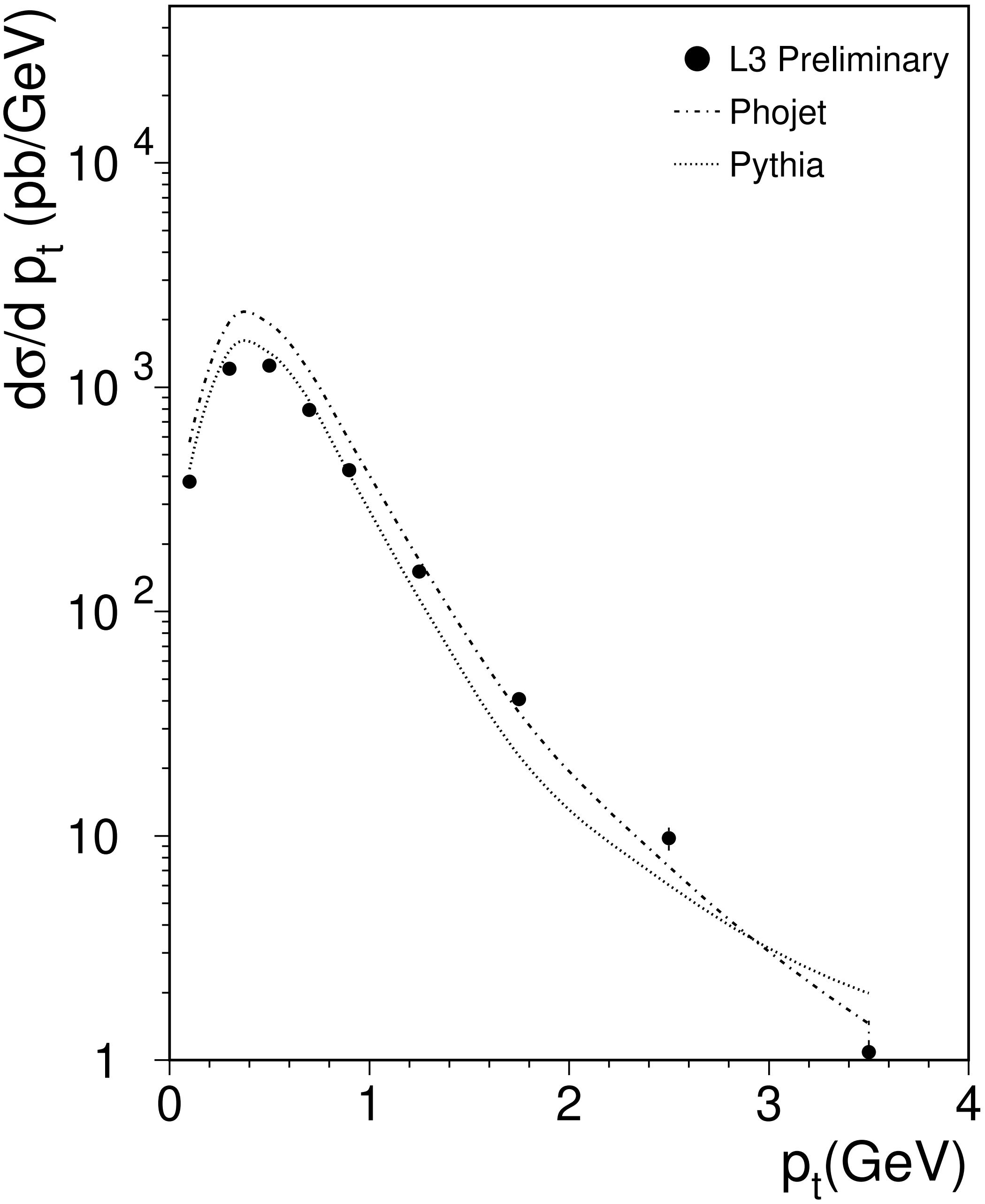

Figure 11: The measured differential cross section as a function of p_t for $|\eta| < 1.5$ is compared to the predictions of the PHOJET and PYTHIA Monte Carlos.

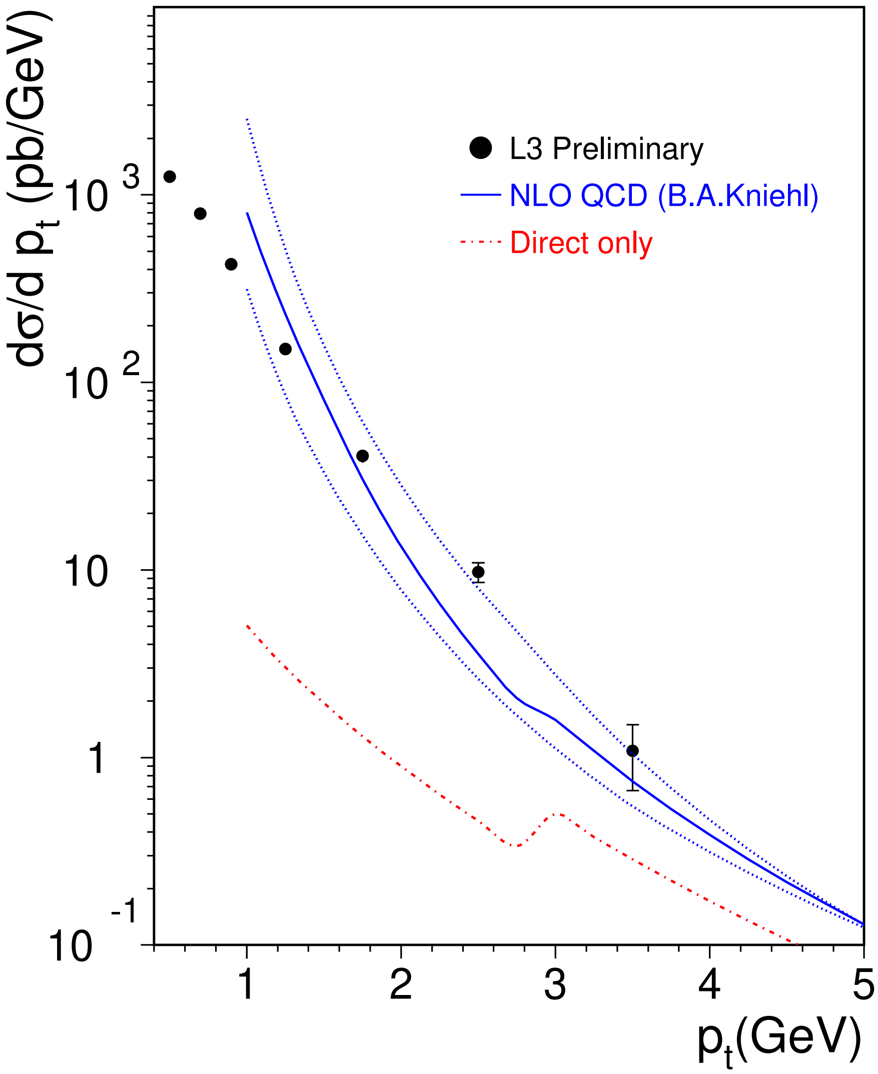

Figure 12: The measured differential cross section as a function of p_t for $|\eta| < 1.5$ is compared to the NLO QCD predictions by B.A. Kniehl. The solid line corresponds to the scale factor (see text) $x = 1$ while the upper dotted line to $x = 0.5$ and the lower dotted line to $x = 2$. The dash-dotted line corresponds to the direct contribution where the distortion at 3 GeV is due to the threshold for charm production.

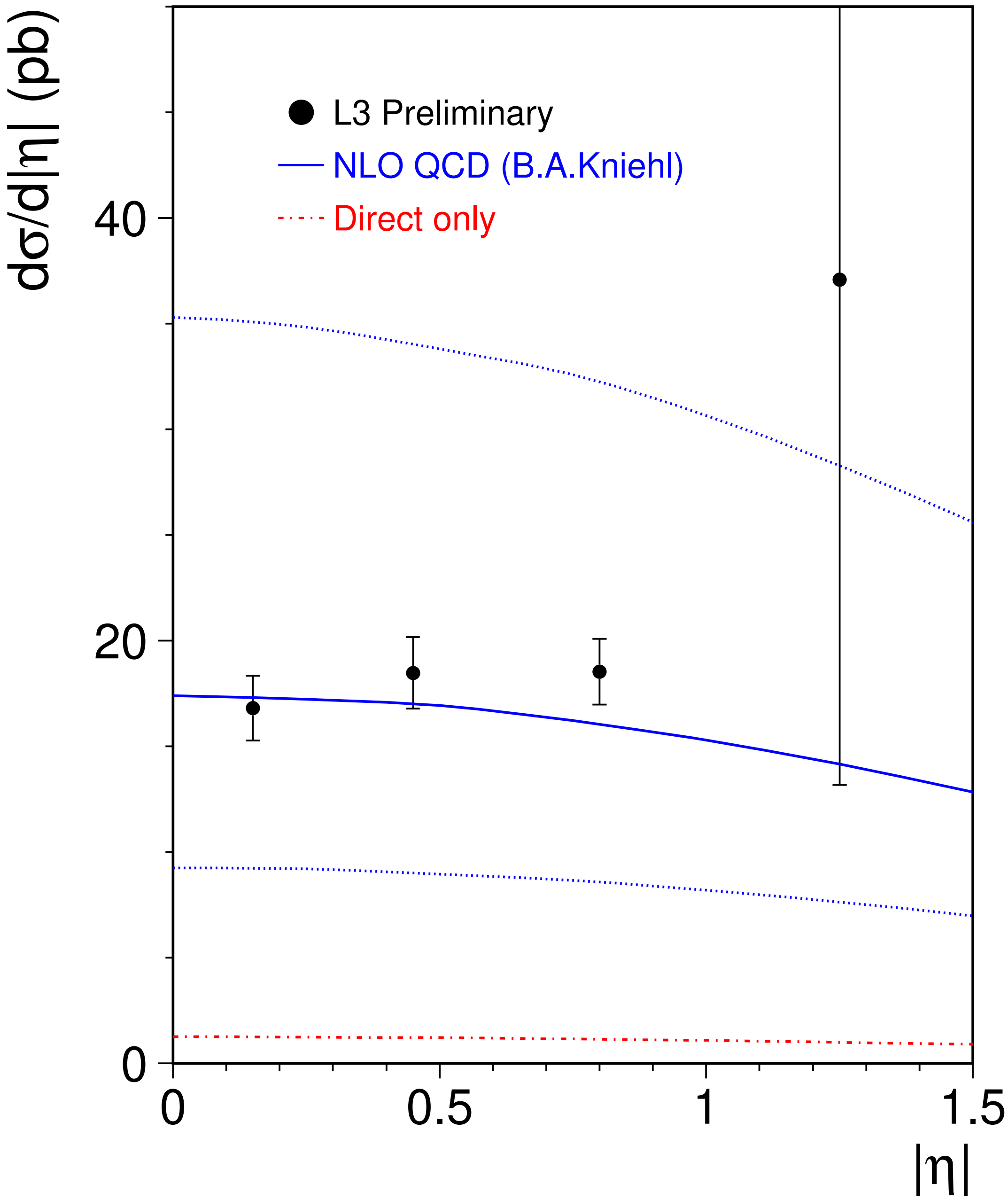

Figure 13: The measured differential cross section as a function of $|\eta|$ for $p_t > 1.5$ GeV is compared to the NLO QCD predictions by B.A. Kniehl. The solid line corresponds to the scale factor (see text) $x = 1$ while the upper dotted line to $x = 0.5$ and the lower dotted line to $x = 2$. The dash-dotted line corresponds to the direct contribution. The large error of the measurement at $|\eta| > 1$ is due to the very limited statistics.

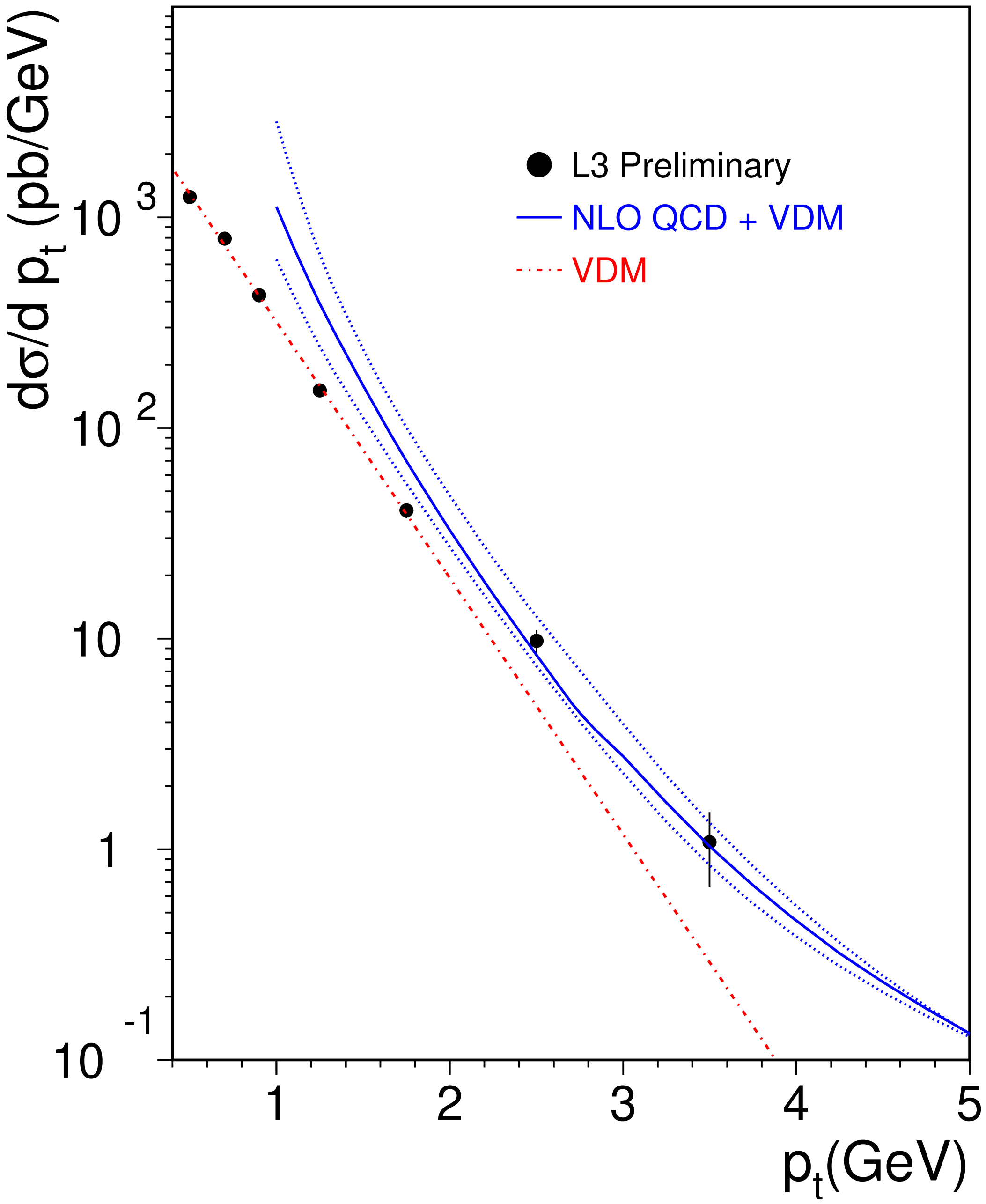

Figure 14: The measured differential cross section as a function of p_t for $|\eta| < 1.5$ is compared to the sum of the NLO QCD predictions and the VDM exponential fit (dash-dotted line). The solid line corresponds to NLO QCD prediction for a scale factor (see text) $x = 1$ while the upper dotted line to $x = 0.5$ and the lower dotted line to $x = 2$.